W. DIETZEL, P. Bala SRINIVASAN
GKSS-Forschungszentrum Geesthacht GmbH, D-21502 Geesthacht, Germany

HYDROGEN EMBRITTLEMENT AND WEAR OF MAGNESIUM ALLOYS

Key words

Magnesium alloys; Hydrogen embrittlement; Plasma electrolytic oxidation; Microstructure; Tribological properties.

Summary

Lightweight combined with good mechanical properties makes magnesium alloys attractive for many applications. However, these alloys have a poor resistance against corrosion. Associated with the corrosion of magnesium alloys is hydrogen embrittlement of the material, since, in the corrosion reaction, atomic hydrogen is generated which partly enters the material and leads to cracking. Another matter of concern for magnesium alloys is their low wear resistance, owing to the inherent low hardness of the material. The influence plasma electrolytic oxidation (PEO) coating on the tribological characteristics of an AM50 magnesium alloy assessed by dry sliding wear tests and the associated wear mechanisms are discussed in this paper.

1. Introduction

Stress corrosion cracking, SCC, is one of the major causes of failure of engineering components and structures made from metallic materials [1]. An important mechanism causing failure is the embrittlement of the material due to the uptake of atomic hydrogen from the environment [2]. Here, fracture mechanics (FM) methodology has proven to be a useful tool for investigating

fracture processes caused by SCC and HE, both theoretically and practically, and for taking into account environmental effects on the fracture process [3].

Magnesium alloys are looked at as potential candidates for lightweight structural constructions. The increasing demand for lighter, more fuel-efficient automobiles has led to renewed interest in the use of these alloys for automobile components. A major barrier, however, to the increased use of Mg alloys for automobile components is their high susceptibility to SCC in common service environments [4].

When subjecting magnesium specimens to constant elongation rate tensile (CERT) tests in distilled water, experimental evidence has shown that the SCC consists of a sequence of film rupture events at the specimen surface, leading to the exposure of bare metal to the aqueous environment. The corrosion of the bare magnesium surface thus exposed to the aqueous environment leads to an electrochemical reaction with the water in which magnesium hydroxide and hydrogen [5].

A part of the atomic hydrogen generated in this reaction recombines hydrogen gas at the specimen surface, which bubbles up in the test solution. Another part of the hydrogen atoms is adsorbed at the specimen surface inside the pit that forms due to the corrosion reaction and enters the bulk of the specimen. Subsequently, the hydrogen atoms diffuse inside the material to the highly stressed regions of the specimen and raise the hydrogen concentration at these sites.

Although there exists a considerable body of research outlining the phenomenology of SCC of Mg alloys, little consensus can be found in the literature regarding the underlying mechanisms [4, 6]. Yet, the development of durable Mg alloys for automobile components would require a profound understanding of these mechanisms.

In addition to the environmentally assisted damage, magnesium alloys, being soft, also have the propensity to undergo mechanical damage, viz. wear. Under such circumstances, surface modification of magnesium alloys with suitable coatings to combat the problem of wear becomes mandatory. A variety of coating technologies, i.e., conversion coatings, vapour deposition, conventional anodising, organic coatings, etc., enhance the corrosion resistance of magnesium alloys [7] but do not greatly influence the wear resistance. The plasma electrolytic oxidation (PEO) technique, which has become popular in recent years, is capable of forming a hard ceramic oxide layer on the surface of magnesium alloys that, in addition to improving the electrochemical characteristics, provides an enhanced tribological behaviour [8–9]. Even though the microstructure-general corrosion behaviour correlation of PEO coated magnesium alloys has extensively been documented, the published information on the wear and SCC behaviour of PEO coated magnesium alloys is very limited [10–13].

Both issues, i.e. the hydrogen assisted cracking behaviour of magnesium alloys and the influence of PEO coatings on their dry sliding wear behaviour, are addressed in this paper.

2. Experimental Details

For the investigations related to hydrogen embrittlement, fatigue pre-cracked C(T) specimens were subjected to increasing displacements - applied in the form of constant extension rates measured in the load-lines of the specimens - while they were exposed to a corrosive environment. The onset and extent of crack growth was monitored using a modified version of the DC potential drop technique. Further details of the experimental setup for the SCC tests and the test technique are given elsewhere [1, 3].

The material used for the HE investigations was a commercial magnesium alloy AZ31 nominally containing about 3 wt-% aluminium and up to 1 wt-% zinc, with the balance being magnesium. The SCC test environment was double-distilled H_2O. The reason for using distilled water instead of a typical corrosion environment, e.g., a chloride containing solution, was due to the severe pitting corrosion which would occur in NaCl solutions and which would override the effect of HE. Control tests were carried out in laboratory atmosphere. The specimens were immersed in the environment to just above the machined notch. The fatigue crack was saturated with distilled water prior to each test by applying a small constant load (~0.5 kN) to the immersed specimen for ~24 h. The distilled water was slowly circulated between the environment cell and a remote reservoir. The applied tensile load was increased under Constant Extension Rate Test (CERT) conditions, with the extension measured using a clip gauge at the crack mouth (CMOD). The tests were conducted at three different extension rates, i.e., 1, 2 µm/h and 100 µm/h, respectively. The tests were evaluated according to linear elastic fracture mechanics methodology, i.e. the stress intensity factor K was calculated at the onset of crack extension using:

$$K = \frac{F}{B\sqrt{W}} \frac{(2+a/W)}{(1-a/W)^{1.5}} [0.886+4.64a/W-13.32(a/W)^2+14.72(a/W)^3-5.6(a/W)^4] \quad (1)$$

where F is the load at crack initiation, W the ligament and a the initial crack length.

For the tribological characterisation, an AM50 magnesium alloy was chosen as the substrate. Specimens of 40 mm x 40 mm x 4 mm were plasma electrolytic oxidation treated using a pulsed DC power source in alkaline phosphate and acidic fluozirconate electrolytes, respectively. The surface roughness of the coatings was assessed using a Hommel profilometer, and the

thickness of the coatings was determined using a MiniTest 2100 meter. X-ray diffraction (XRD) was performed using a Philips PW1820 diffractometer with Cu-Kα radiation to determine the phase composition of the PEO coatings. Scanning electron microscopy (SEM) was used to examine the surface morphology of the PEO coatings.

The tribological characteristics of the untreated and PEO coated specimens was assessed using a Tribotec ball-on-disc tribometer with an AISI 52100 steel ball of 6 mm diameter as a static friction partner. The dry sliding wear tests were performed at ambient conditions (22±2°C) under 2N with a sliding amplitude of 10 mm and at a velocity of 5 mm s^{-1}, for a distance of 50 m. Wear depth measurements were performed with the Hommel profilometer. The worn balls and the wear tracks were examined and characterised by energy dispersive spectroscopy in a Zeiss Ultra 55 SEM.

3. Results and discussion

3.1. Hydrogen embrittlement

As can be seen from the comparison between a specimen tested in laboratory atmosphere and one tested in distilled water shown in Fig. 1, a single, sharp stress corrosion crack extended from the tip of the fatigue crack, through the entire width of the specimen, and propagated perpendicular to the loading direction.

Fig. 1. Comparison of a AZ31 C(T) specimens tested in laboratory atmosphere (left) and in the distilled water (right)

In Fig. 2, the results of the fracture mechanics based SCC tests on the pre-cracked C(T) specimens are displayed. The values of the stress intensity factor, K_I, are plotted as a function of the crack mouth opening displacement, CMOD up to the point at which crack initiation occurred, detected by a sharp increase in the DCPD signal. Although the overall slopes of the curves appear to some

extent similar, it is obvious that in distilled water, i.e. under the condition of hydrogen embrittlement, the cracks initiated at much lower values of the CMOD than in the reference tests in air. In the tests performed at the two extension rates, 1 and 2 µm/h, cracking was observed after less than a 0.5 mm increase in CMOD, corresponding to a test duration of about 300 hours. In a specimen tested in air at the same extension rate of 2 µm/h, cracking occurred only after more than 2100 hours and after CMOD values of 3 to 5 mm. At the higher extension rate of 100 µm/h, the fracture behaviour was obviously not significantly influenced by the respective test environment. In distilled water, the mechanical rupture had obviously overridden the degradation effect caused by the hydrogen uptake.

The initial gradients of the K_I versus CMOD curves for AZ31 were obviously not strongly affected by the corrosive environment. (Fig. 2) The reduction in the gradient in the presence of distilled water was only marginal, even though, unlike the tests in air, there was no visible plastic deformation on the plane surface of the specimens (Fig. 1).

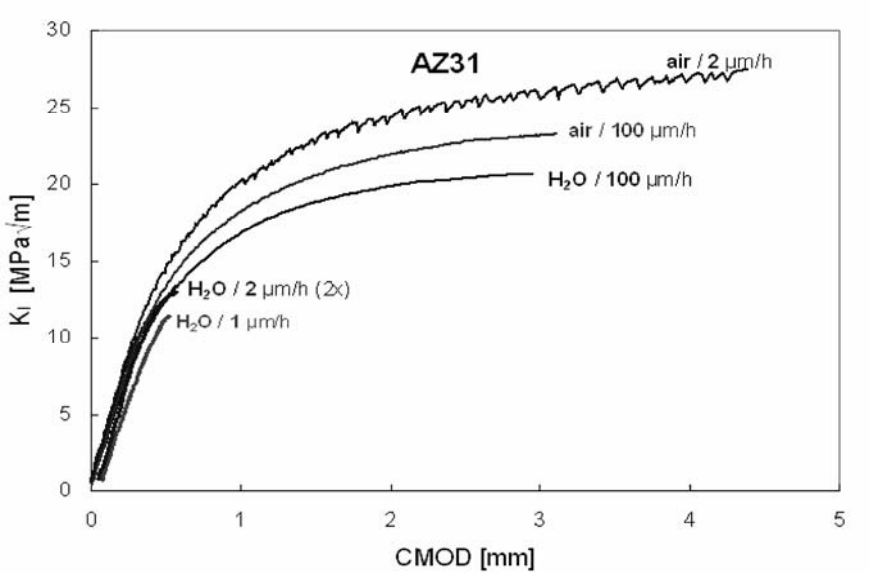

Fig. 2. Curves of the stress intensity factor, K_I, versus crack mouth opening displacement, CMOD, measured in tests on pre-cracked C(T) specimens of the Mg alloy AZ31, plotted up to the onset of cracking determined by a drop in the DCPD signal

The K_{ISCC} values determined from the DCPD measurements (Fig. 2) for AZ31 lies in the order of 11 MPa√m; hence, it is in the range of values by given other workers for Mg alloys (see in [4]). Since the value of K_{ISCC} is dependent

on the propensity for film breakdown and H ingress at the crack tip and given that distilled water does not promote localised corrosion in AZ31, this implies that the measured K_{ISCC} may not be the minimum value for AZ31. It is likely be further reduced by using a slightly more aggressive environment which promotes hydrogen generation and uptake more strongly.

Fig. 3 shows a comparison of typical morphologies of the fracture surfaces of the specimens tested in laboratory atmosphere and in distilled water. The fracture surfaces produced in air (left side of Fig. 3) were characterised by coarse, irregular dimple-like features. Similar features were observed in the areas of the final overload fracture of the specimens tested in distilled water at low displacement rates. The fracture surfaces of these latter specimens comprised SCC zones with fluted regions, as can be seen on the right side of Fig. 3.

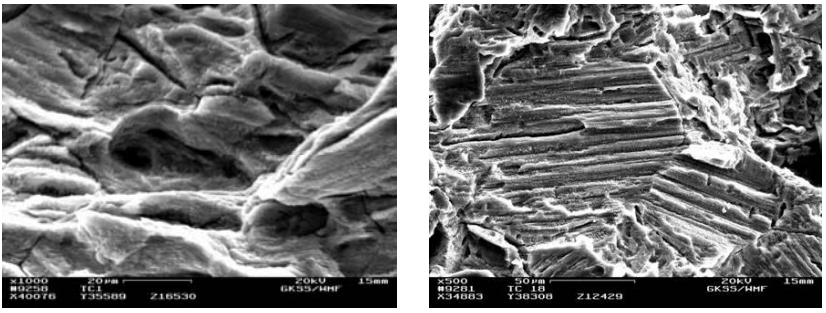

Fig. 3. Morphology of the fracture surfaces of the specimens shown in Fig. 1

3.2. Wear behaviour

3.2.1. Microstructure of PEO coated magnesium alloy

Optical micrographs revealing the surface and cross-sectional morphologies of the two PEO coatings are shown in Fig. 4. The coating obtained from the phosphate electrolyte was found to be constituted only with MgO, and the coating obtained from the acidic zirconate electrolyte contained predominantly ZrO_2 and small amounts of MgF_2 and MgO. The coatings from phosphate and zirconate electrolytes shall hereinafter be addressed as MgO and ZrO_2 coatings, respectively.

The morphology of MgO coating presented in Fig. 4(a) reveals a surface with numerous pores of different sizes. The mean surface roughness (R_a) of the MgO coating was 2.2±0.2 μm. The ZrO_2 coating shown in Fig. 4(c) had a different surface appearance compared to the MgO coating. The surface contained some sintered protrusions with relatively large-sized micropores and large regions of numerous smaller micropores. Due to the above morphological

features, the surface of the ZrO_2 coating was very rough which was confirmed by the roughness measurements (R_a = 3.6±0.6 μm).

The cross-section morphology of the MgO coating shown in Fig. 4(b) reveals spherical pores, some of which were filled with coating compounds, and a few others were like gas bubbles. The thickness of the MgO coating was 28±5 μm. On the other hand, the ZrO_2 coating was 40±8 μm thick (Fig. 4(d)) and, unlike in the case of the MgO coating, the cross-section of the ZrO_2 coating contained relatively large irregular-shaped pores and micro-cracks and this coating had a sponge-like structure.

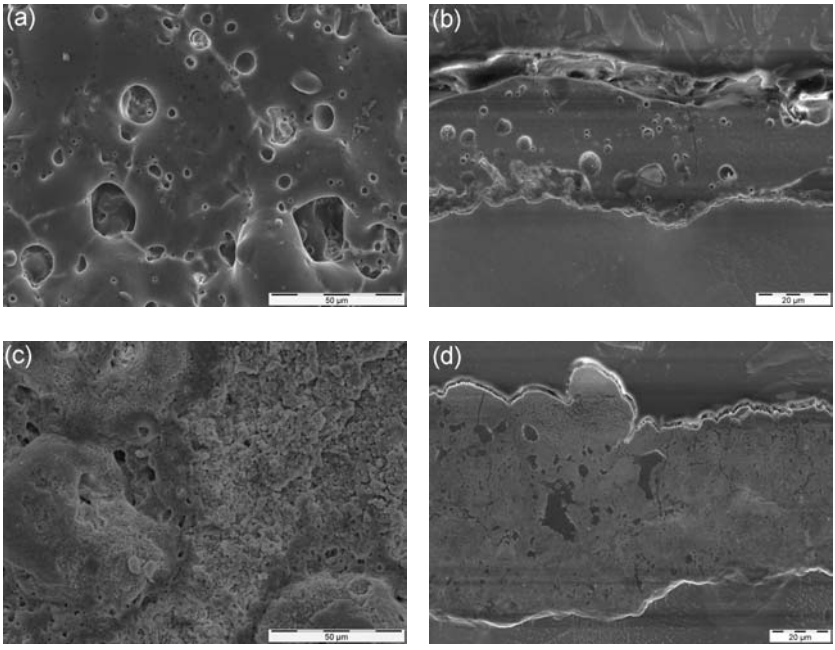

Fig. 4. Surface and cross-sectional morphologies the PEO coated AM50 magnesium alloy (a) & (b) MgO and (c) & (d) ZrO2 coated

3.2.2. Dry sliding wear behaviour

The variation of friction co-efficient in the oscillating dry sliding wear tests involving the untreated/PEO coated magnesium substrates and AISI 52100 steel ball under 2 N load is shown in Fig. 5. A friction co-efficient value in the range of 0.28–0.32 was registered for the untreated magnesium alloy-steel sliding couple. On the other hand, much higher friction co-efficient values were registered during the sliding of MgO and ZrO_2 coated magnesium alloy specimens against the steel ball. For the MgO coated specimen, the friction co-efficient value rose steadily to a value of about 0.73±0.02 in about 15 m of

sliding and remained steady thereafter until the test was terminated after 50 m of sliding. In the case of the ZrO_2 coated specimen, the friction co-efficient value rose instantly to around 0.70. The value increased further to reach a steady-state value of 0.82 $\pm$ 0.02 during 5 m and 40 m of sliding. After this point, a few sharp fluctuations were observed. Nevertheless, the value remained above 0.70 until the test was terminated after 50 m of sliding. Jun et al. have observed a friction co-efficient value in the range of 0.60–0.70 for a PEO coating which was constituted predominantly with MgO when slid against a Si_3N_4 ceramic ball [11]. A higher friction coefficient (0.70 – 0.80) value was observed for a silicate PEO coated Mg alloy and steel couple in yet another work of our group [14].

The scanning electron macrographs of wear tracks of the untreated AM50, MgO and ZrO_2 coated magnesium alloy specimens are shown in Figs. 6 (a), (b) and (c), respectively. The wear track on the untreated magnesium specimen had deep scoring marks in the direction of sliding, and the surface was covered with metallic and oxide wear debris (Fig. 6(a)). Whilst the coating in the wear track of the MgO coated specimen was more or less intact (Fig. 6(b)), the coating in the wear track of ZrO_2 coated specimen was found to have been removed completely during the wear test (Fig. 6(c)).

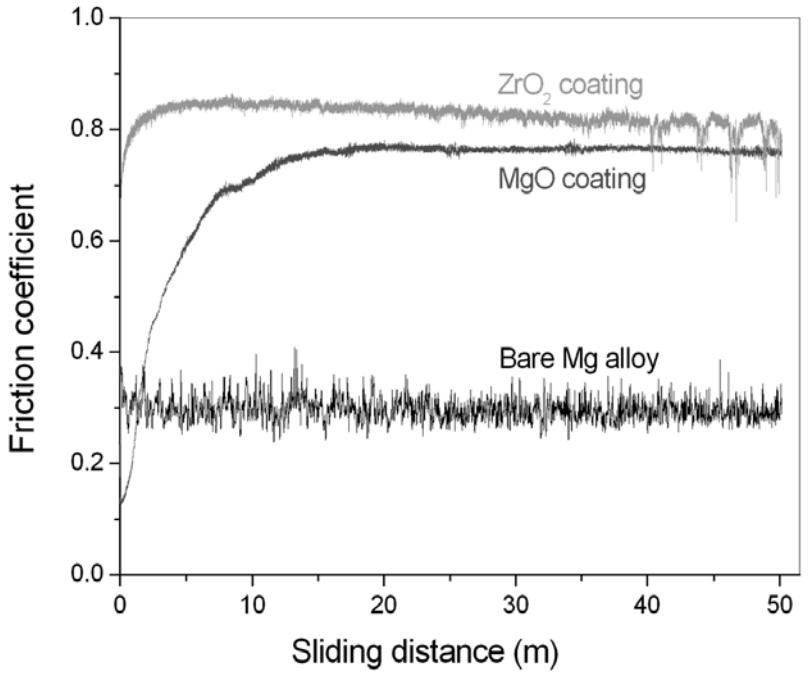

Fig. 5. Variation of friction co-efficient as a function of sliding distance in the dry sliding wear tests against AISI 52100 steel ball

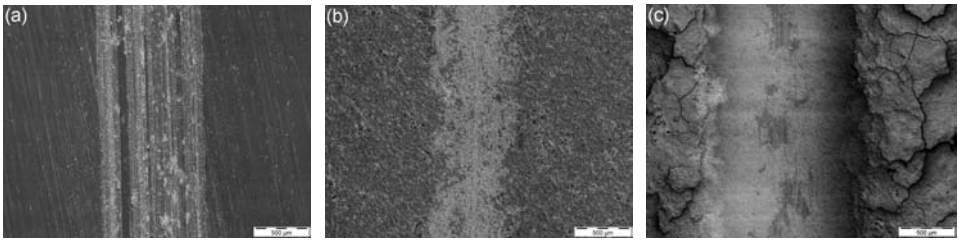

Fig. 6. Wear tracks of the (a) untreated (b) MgO coated and (c) ZrO2 coated magnesium alloy specimens slid against steel ball under 2N load

The specific wear rates of the untreated alloy and the MgO and ZrO_2 coated magnesium substrates were 1.8 x 10^{-3} mm³ N^{-1} m^{-1}, 2.4 x 10^{-4} mm³ N^{-1} m^{-1} and 5.0 X 10^{-3} mm³ N^{-1} m^{-1}, respectively. In an earlier work, it had been found that the wear resistance of the PEO coating obtained from phosphate electrolyte was inferior to that of coatings produced from a silicate based electrolyte [21]. However, amongst the two coatings produced in this work, the one from the phosphate electrolyte was found to exhibit a better wear resistance on account of its higher compactness. The poor wear resistance of the ZrO_2 coating was attributed to its porous and spongy structure.

The scanning electron macrographs of the surfaces of the corresponding counterpart (steel ball) surfaces are shown in Figs, 7(a), (b) and (c), respectively. The steel ball that slid against the untreated magnesium alloy did not show any signs of wear damage. The contact region marked in circle in Fig. 7(a) shows that the surface was covered with transferred wear debris from the magnesium alloy. The steel ball did not undergo any visible wear damage; however, due to the adhesive wear mechanism that prevailed at the interface, transfer of debris from the magnesium substrate to the steel ball had resulted as can be seen in Fig. 7(a).

In the case of the steel ball slid against the MgO coated magnesium alloy, an abrasive wear damage was noticed on the steel ball surface (Fig. 7(b)) with the ball showing a specific wear rate of 6.8 x 10^{-5} mm³ N^{-1} m^{-1}. As mentioned earlier, there was only a very little wear damage to the MgO coated magnesium alloy counter surface. On the contrary, the surface of the steel ball slid against the ZrO_2 coated magnesium alloy did not undergo any wear damage (Fig. 7(c)). The original spherical shape of the ball at the contact surface remained intact, as was also observed in the case of the ball slid against the untreated magnesium alloy. However, some wear debris observed on this surface was found to have transferred from the ZrO_2 coated surface, as ascertained by EDS measurements. The results showed that the dry sliding wear resistance of the AM50 magnesium alloy substrate can be improved with the application of a compact PEO coating possessing a good load bearing capacity. By the same token, the studies also

demonstrated that a coating with sponge like structure even with a higher thickness can adversely influence the wear behaviour.

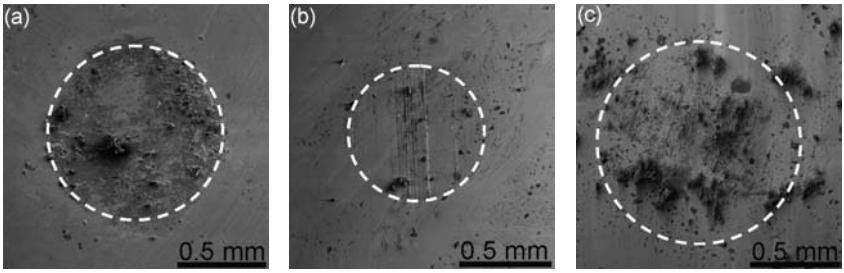

Fig. 7. Surface appearances of the worn steel balls slid against (a) untreated, (b) MgO coated and (c) ZrO2 coated magnesium alloy specimens

Conclusions

The magnesium alloy AZ31 is susceptible to hydrogen embrittlement in distilled water when being subjected to test under monotonically increasing extension. Fracture mechanics SCC tests on pre-cracked C(T) specimens allow the determination of threshold value K_{ISCC} for the onset of cracking due to HE.

AM50 magnesium alloy undergoes an adhesive wear when slid against a steel ball in the dry sliding wear tests under 2N. A relatively compact, dense, 30 µm PEO coating with MgO as the major phase composition could provide a very good wear resistance to the magnesium substrate. Despite a higher thickness, the ZrO_2 containing PEO coating on the magnesium substrate could not provide a protection against wear due to the spongy structure. The three body abrasive wear that gets set-up by the entrapment of wear debris in the sliding couples involving the ZrO_2 coated specimen had led to a higher specific wear rate of the coated alloy than the untreated substrate. Even though the phase composition and the thickness of the PEO coatings can influence the wear resistance, the compactness, the defect levels and the load bearing capacity of the coatings dictate the wear performance of the coated magnesium alloys under dry sliding conditions.

References

1. W. Dietzel, A. Turnbull, Stress Corrosion Cracking. in: K.-H. Schwalbe (Ed.), Comprehensive Structural Integrity, Addendum 2007: Mechanical Characterization of Materials. Oxford UK: Elsevier (2007) 43–74.
2. M. Gao, R.P. Wei, Met. Trans. A16 (1985) 2039.

3. W. Dietzel, M. Pfuff, The Effect of Deformation Rates on Hydrogen Embrittle-ment, in: Hydrogen Effects in Materials, A.W. Thompson, N.R. Moody (Eds.), TMS, Warrendale, PA (1996) 303–311.
4. N. Winzer, A. Atrens, G. Song, E. Ghali, W. Dietzel, K.U. Kainer, N. Hort, C. Blawert, Adv. Eng. Mater. 8 (2005) 659.
5. A. Atrens, W. Dietzel, Adv. Eng. Mat. 9 (2007) 292.
6. N. Winzer, A. Atrens, W. Dietzel, K.U. Kainer, Met. Trans. A39 (2008) 1157.
7. J.E. Gray, B. Luan, J. Alloys Compd. 336 (2002) 88.
8. C. Blawert, W. Dietzel, E. Ghali, G. Song, Adv. Eng. Mater. 8 (2006) 511.
9. P. Bala Srinivasan, C. Blawert, M. Störmer, W. Dietzel, Surf. Eng. DOI 10.1179/174329409X379246.
10. K.C. Goretta, A.J. Cunningham, N. Chen, D. Singh, J.L. Routbort, R.G. Rateick Jr, Wear, 262 (2007) 1056.
11. J. Liang, L. Hu, J. Hao, Appl. Surf. Sci. 253 (2007) 4490.
12. P. Bala Srinivasan, C. Blawert, W. Dietzel, Mat. Sci. Eng. A494 (2008) 401.
13. P. Bala Srinivasan, C. Blawert, W. Dietzel, Corros. Sci. 50 (2008) 2415.
14. P. Bala Srinivasan, C. Blawert, W. Dietzel, Wear, 266 (2009) 1241.

Reviewer:
Lech STARCZEWSKI

Kruchość wodorowa i zużycie stopów magnezu

Słowa kluczowe

Stopy magnezu, kruchość wodorowa, mikrostruktura, właściwości tribologiczne, utlenianie elektrolityczno-plazmowe.

Streszczenie

Niska waga połączona z dobrymi właściwościami mechanicznymi czynią stopy magnezu atrakcyjnymi w wielu zastosowaniach. Jednak stopy te wykazują niską odporność na korozję. Z korozją związana jest kruchość wodorowa stopów magnezu, wynikająca z wydzielaniem w trakcie reakcji korozyjnych wodoru atomowego, który częściowo wnika do materiału i prowadzi do pękania.

Kolejnym zagadnieniem jest niska odporność stopów magnezu na zużycie cierne. W pracy przedstawiono wpływ utleniania plazmowo-elektrolitycznego (PEO) na charakterystykę tribologiczną stopu AM58 w warunkach tarcia suchego oraz związane z nią mechanizmy zużycia.